Roentgen stereophotogrammetric analysis to study dynamics and migration of stent grafts

Koning, O.H.J.

CHAPTER

4

Accurate Detection of Stent-Graft Migration in a Pulsatile Aortic Model Using Roentgen Stereophotogrammetric Analysis

Olivier H.J. Koning
Eric H. Garling
Jan-Willem Hinnen
Lucia J.M. Kroft
Edwin van der Linden
Jaap F. Hamming
Edward R. Valstar
and J. Hajo van Bockel

J Endovasc Ther 2007;14:30–38

Abstract

Purpose: To evaluate the feasibility and accuracy of Roentgen stereophotogrammetric analysis (RSA) versus computed tomography (CT) for detecting stent-graft migration in an in vitro pulsatile circulation model and to study the feasibility of a nitinol endovascular clip (NEC) as an aortic wall reference marker for RSA.

Methods: An aortic model with stent-graft was constructed and connected to an artificial circulation with a physiological flow and pressure profile. Tantalum markers and NECs were used as aortic reference markers for RSA analysis. Stent-graft migrations were measured during pulsatile circulation with RSA and CT. CT images acquired with 64×0.5-mm beam collimation were analyzed with Vitrea postprocessing software using a standard clinical protocol and central lumen line reconstruction. RSA in the model with the circulation switched off was used as the reference standard to determine stent-graft migration. The measurement errors of RSA and CT were determined during pulsatile circulation.

Results: The mean measurement error ± standard deviation (maximum) of RSA during pulsatile circulation using the tantalum markers was –0.5±0.16 (0.7) mm. Using the NEC, the mean (maximum) measurement error was –0.4±0.25 (1.1) mm. The mean (maximum) measurement error of CT was –1.1±1.17 (2.8) mm.

Conclusion: RSA is an accurate and feasible tool to measure stent-graft migration in a pulsatile environment. Migration measurement with RSA was more accurate than CT in this experimental setup. The nitinol clip tested in this study is potentially feasible as an aortic reference marker in patients after endovascular repair.

Introduction

Stent-graft migration is a potential complication after endovascular aneurysm repair (EVAR) of an abdominal aortic aneurysm (AAA) .[1-3] Periodic surveillance is necessary to detect migration and other complications.[4,5] The current gold standard for follow-up after EVAR is contrast-enhanced computed tomography (CT).[6] However, this modality requires intravascular contrast, a high radiation dosage, and significant logistical consequences and costs, making EVAR less cost effective.[7] For these reasons, the use of CT for routine surveillance after EVAR is less attractive. Reducing the frequency of CT imaging in EVAR surveillance may be possible, especially if there is evidence of sac shrinkage.[8] However, stent-graft migration may go unnoticed as a result of this reduced imaging frequency.

Roentgen stereophotogrammetric analysis (RSA) may be a valuable alternative to identify stent-graft migration.[9] This technique is a well established and highly accurate tool to detect 3-dimensional micromotion of orthopedic implants in relation to tantalum reference markers in the bone.[9-13] The potential benefits of RSA are low costs, low radiation dose, and no intravenous contrast enhancement. In addition to these potential benefits of RSA, its highly accurate method of measurement could be of great advantage in detecting migration in the early period after introduction of new endografts.

Furthermore, RSA data acquisition and analysis is simple and fast and can be performed by a trained technician. Since RSA images are stereo plain abdominal radiographic images, they can also be used to detect stent fractures. In a static model for stent-graft migration, RSA was found to be more accurate than CT.[9]

A disadvantage of RSA is that aortic wall reference markers are required to assess the relative motion of the stent compared to the aorta.[9] The pulsatile change of the aortic diameter results in movement of both the aortic markers and stent-graft markers during the cardiac cycle, which could induce a measurement error in RSA.

In this study, we evaluated the effect of pulsatile motion on the accuracy of RSA and CT in stent-graft migration measurement in an in vitro model for endograft migration with physiological flow and pressure profiles. Furthermore, we tested the feasibility of a nitinol endovascular clip (NEC) as an aortic reference marker for RSA.

Methods

Pulsatile Aortic Model With Stent-Graft

A pulsatile flow model was developed to simulate migration of a stent-graft in the pulsating aorta. A human cadaver spine was obtained from the anatomical department and used according to the standard consent procedures of our Institutional Review Board. A fresh specimen of a pig thoracic aorta was attached to the cadaver spine, replacing the cadaveric aorta. The spine, including the surrounding soft tissues, was conserved in a solution of formaldehyde, ethanol, glycerin, and phenol (Figure 1). Since accurate CT analysis requires a reference point (usually a renal artery), a side branch was anastomosed to the aorta at the level of the cadaver's renal artery. The model was placed in a Plexiglas box, topped off with water to simulate soft tissue. The perfusate of this artificial circulation was starch solution with the same viscosity as blood. To enable CT analysis, the perfusate was enhanced with intravascular contrast [iomeprol 816.5 mg/mL (Iomeron 400); Altana Pharma, Hoofddorp, The Netherlands) to a level of 250 Hounsfield units, which is similar to the attenuation in a normal abdominal CT scan. The

Figure 1. The porcine aorta fixed to the human cadaveric spine. A side branch was attached to the aorta at the site of the original renal artery. Cranial side to the left.

contrast was washed out by changing the perfusate after each CT acquisition, so RSA imaging was not disturbed by the contrast medium.

To generate pulsatility, the model was connected to an artificial circulation set at 70 beats per minute with a 75 mL/s flow rate, which produced a physiological flow and pressure profile (Figure 2 and 3).[14] The pulsatility resulted in a luminal diameter change from 20.0 to 21.5 mm, as recorded in M-mode ultrasound with a 7.5-MHz linear array probe (ProSound SSD-5500; ALOKA, Tokyo, Japan). This diameter change was induced to simulate aortic diameter changes measured in vivo.[16-18]

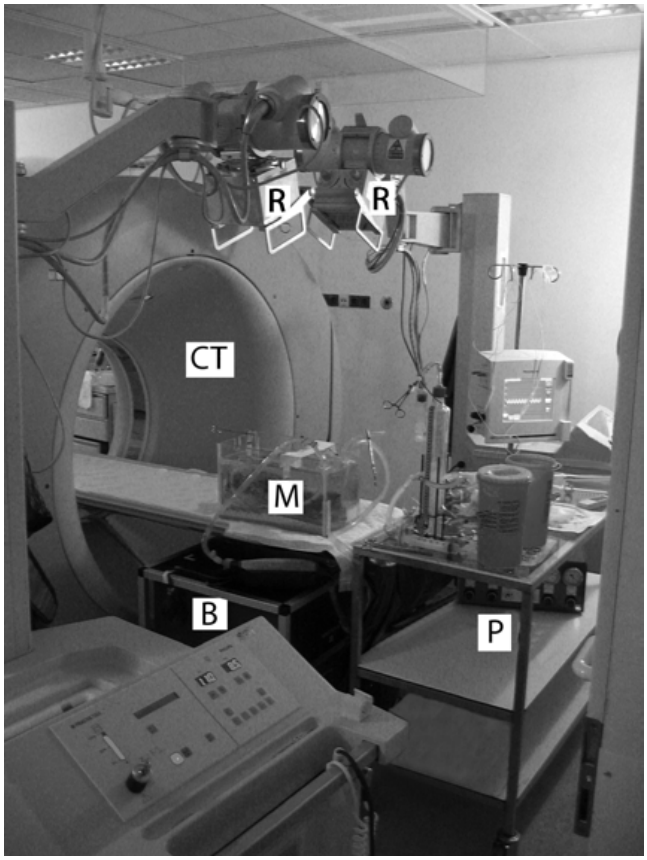

Figure 2. Experimental setup. The model (M) is placed on the CT table. Imaging can be switched between RSA and CT without disturbing the model. The physiological flow and pulsatility is generated with an artificial circulation (P). The RSA setup is positioned next to the CT gantry (CT). Two crossing X-ray beams from the 2 Roentgen foci (R) expose the films under the calibration box (B).

A Gianturco stent (Cook, Bjaeverskov, Denmark) was placed inside the aorta (Figure 4). A stent rather than a stent-graft was used to model migration since radiological imaging techniques use the stents of the stent-graft for analysis. Furthermore, deleting the fabric from the model facilitated the induction of migration. The stent could be "migrated" along the aorta by pulling

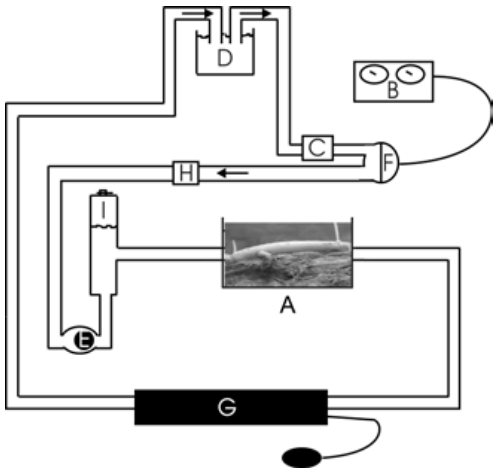

Figure 3. Schematic representation of the model, which consists of the aortic model with stent-graft (A), an artificial heart driver (B), a valve (C), an open reservoir (D), a ball valve (E), left ventricle (F), a blood pressure cuff (G), a flow transducer (H), and an air chamber (I). Fluid pressures were measured at the entrance of the aortic model.

Figure 4. 3D maximum intensity projection of the CT image of the model. Short arrow lower left: tantalum marker; short arrow upper left: nitinol clip; long arrow lower right: renal artery. Cranial side to the left.

on monofilament fishing wire (Spro, Vianen, The Netherlands), which was attached to each side of the stent. To prevent unintended migration, the fishing wire was fixed to the box during the measurements.

For RSA analysis, markers were added at the cranial and caudal corners of the stent (i.e., *stent-graft markers*), and reference markers were attached to the aorta (i.e., *aortic markers*). Two sets of *aortic markers* were tested: (1) 3 clusters of 1-mm-diameter tantalum markers glued to the aortic adventitia with Histoacryl (B. Braun Aesculap, Tuttlingen, Germany), representing the standard clinical RSA situation used in orthopedics (Figure 4), and (2) 3 Anson Refix nitinol endovascular clips (NEC; Figure 5) (Lombard Medical, Didcot, UK) placed in the aortic wall by an endovascular technique to mimic the clinical situation (Figure 4).

Three stent-graft positions were analyzed with RSA and CT: the initial or reference position and 2 migrations. The stent-graft was migrated caudally under visual control provided by an image intensifier (Philips BV300 plus; Philips Medical Systems Europe, The Netherlands).

Figure 5. Nitinol endovascular clip.

RSA Imaging Technique

Two manually synchronized, standard, mobile Roentgen tubes (Philips Practix 2000; Philips Medical Systems Europe) were set to 110 kV/8.5 mAs, resulting in an exposure time of 78 ms for all RSA images. A calibration box was positioned between the model and the radiographic films to define a 3D laboratory coordinate system and to determine the position of the Roentgen foci (Figure 6 and 7).[9] Defining the 3D laboratory coordinate system in each RSA image eliminates any influence of model (or patient) positioning on the outcome of RSA measurements (Figure 8). After digitizing the films, image postprocessing was performed on a personal computer with the help of RSA-CMS software[11-13,15] (MEDIS, Leiden, The Netherlands).[9] The RSA images were randomly numbered, and the reviewer was blinded to the degree of induced migration. Using this technique, it was possible to calculate the distance between 2 groups of markers. Migration was determined by comparing an initial reference RSA image to the follow-up RSA image.

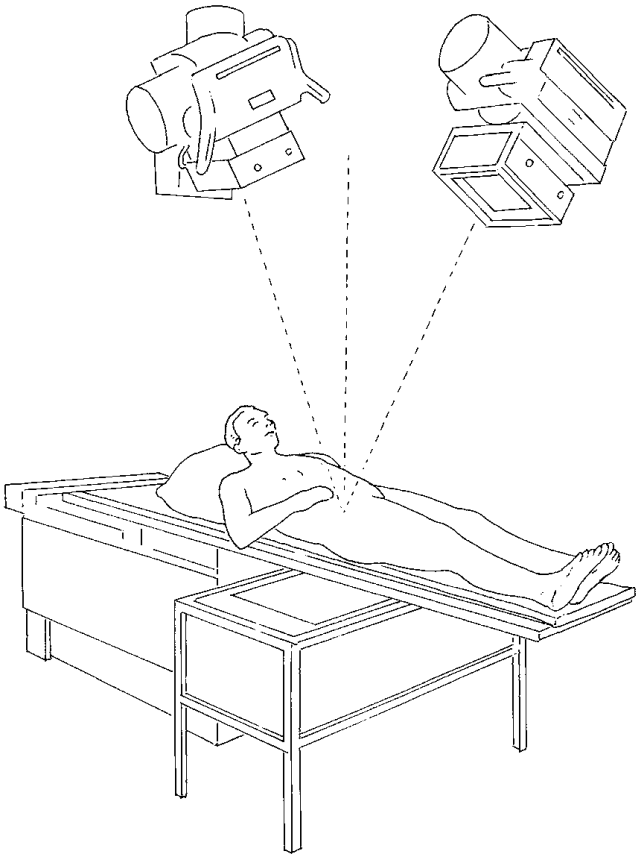

Figure 6. RSA imaging setup. The box under the patient contains markers that are used to define the Roentgen setup and measurement coordinates. The radiographic films are placed directly under the box.

Since RSA is proven to be highly accurate in a static environment,[9-13] RSA of the model without pulsatile circulation was used as the reference standard to determine actual stent-graft migration,[9] using the tantalum aortic reference markers for the analysis. Five RSA images of the reference position and 3 images of each stent-graft position after migration were acquired. These results would later be compared to RSA and CT analysis with pulsatile circulation in the model to determine the measurement error of the 2 techniques. The migration was assessed using cross-table analysis, comparing each of the 5 reference images to all 3 follow-up images, producing 15 measurements per migration.

To determine the influence of pulsatility on RSA migration measurement, 11 RSA images were acquired of each stent-graft position at a random point in the pulsatile circulation cycle. Migration was determined by cross-table analysis, comparing each of the 11 reference images to all 11 follow-up images, resulting in 121 measurements per migration or 121 possible clinical combinations of RSA images. The measurements were performed using tantalum markers as well as NECs. The measured migration with RSA was compared to the actual migration to determine the measurement error of RSA with both types of aortic reference markers.

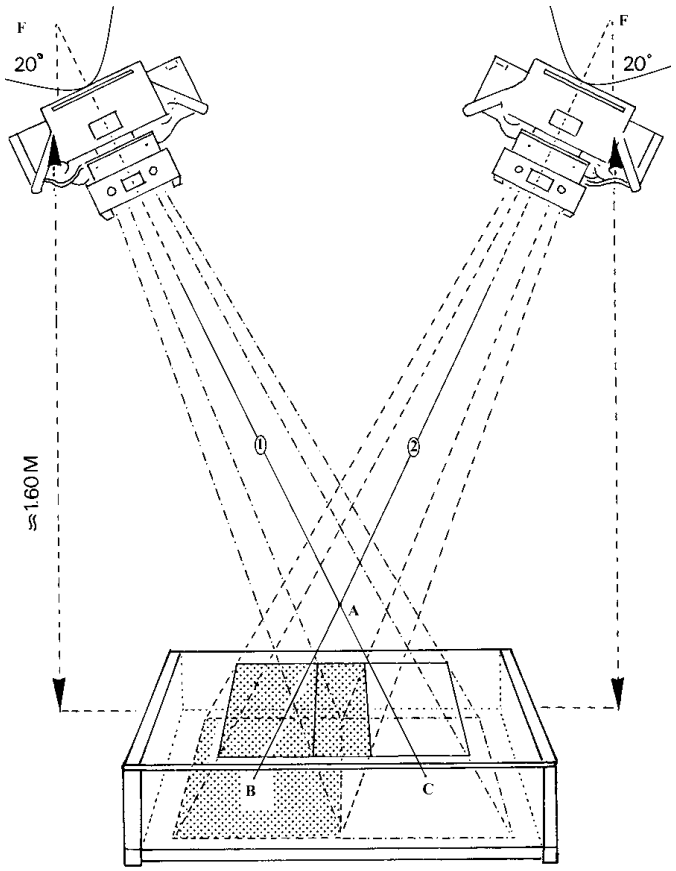

Figure 7. Schematic drawing of the RSA technique. The projection of the calibration box markers on the film is used to reconstruct the position of the Roentgen foci (F). Graft marker A gives projections B and C on the films. With known focus position, projection lines 1 and 2 can be reconstructed; calculating the intersection of 1 and 2 in space gives the position of A.

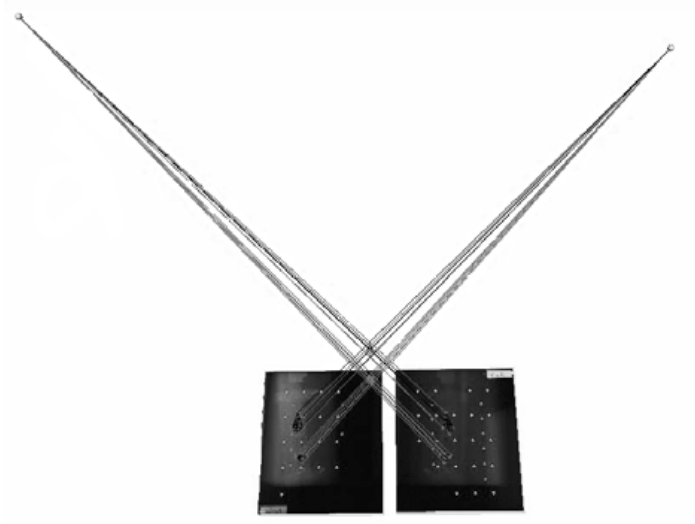

Figure 8. RSA software reconstruction of the position of the 2 Roentgen foci and the stent-graft markers and reference markers in space (crossing lines). These positions were reconstructed from the 2 radiographic images (black).

Computed Tomography

To compare the results of RSA to those of CT, the accuracy of CT measurement with 3D image reconstruction was determined using the same technique for postprocessing and analysis to measure stent-graft position as the one used for CT surveillance in our clinic. The CT images were acquired with a Toshiba Aquilion 64 CT scanner (Toshiba Medical Systems, Otawara, Japan), which was set to 120 kV, 250 mA, 400-ms rotation, pitch factor 0.84, 0.5-mm beam collimation, and 64 detector rows during pulsatile flow in the model. The images were reconstructed with a 0.5-mm thickness and 0.4-mm reconstruction interval.

A reference CT scan was made of the initial stent-graft position. After each migration, a follow-up CT scan was produced. The CT images were randomly numbered, and the observers were blinded to the amount of migration induced. Using Vitrea2 postprocessing software (Vital Images Inc., Plymouth, MN, USA), the amount of migration was measured on 3D curved multiplanar reconstructions along the aortic central lumen line to evaluate the aorta in 2 perpendicular longitudinal directions as well as the perpendicular axial direction. Using automatic calipers, the distance was measured between the lower margin of the renal artery (reference point) and the stent at the level where the first circumferential view of the stent was observed (in perpendicular axial direction). The struts of the stent were used for orientation; no special markers were used for CT measurement.

The CT scans were evaluated by 5 observers: 4 interventional radiologists and a vascular surgeon, all experienced users of this technique. Migration was determined by comparing the distance measured by the same observer in the follow-up CT images to the distance in the reference CT. The resulting migration was compared to the actual migration to determine the measurement error of CT.

Statistical Analysis

Data are presented as the mean ± standard deviation (SD) and maximum. Levene's test for variance was used to detect statistically significant interobserver variability between the measurement errors of the 5 CT readers. The tests were performed using SPSS for Windows (version 11.0; SPSS Inc., Chicago, IL, USA).

Results

The actual migration of the stent-graft as determined by RSA without pulsatile circulation was 7.0±0.02 mm for the first migration (n=15) and 13.9±0.03 mm for the second migration (n=15). For the first migration measured during pulsatile flow (n=121), the mean distance was 6.5±0.08

mm measured by RSA using the tantalum aortic reference markers, which gave a mean (maximum) measurement error of –0.5±0.08 (0.7) mm. For the second migration measured during pulsatile flow (n=121), the mean measured distance was 13.4±0.21 mm, for a mean (maximum) measurement error of –0.5±0.21 (0.7) mm. The pooled error of all migration measurements by RSA in the pulsatile situation using tantalum aortic markers (n=242) was –0.5±0.16 mm (maximum error 0.7 mm). (Figure 9)

Using the NECs as aortic reference markers, the mean distance of the first migration (n=121) measured by RSA was 6.7±0.19 mm [–0.3±0.19 (0.7) mm mean (maximum) measurement error]. The mean distance of the second migration (n=121) was 13.3±0.24 mm [—0.6±0.24 (1.1) mm mean (maximum) measurement error]. The pooled measurement error of all migration measurements by RSA in the pulsatile situation using NECs as reference markers (n=242) was –0.4±0.25 mm (maximum error 1.1 mm). (Figure 9)

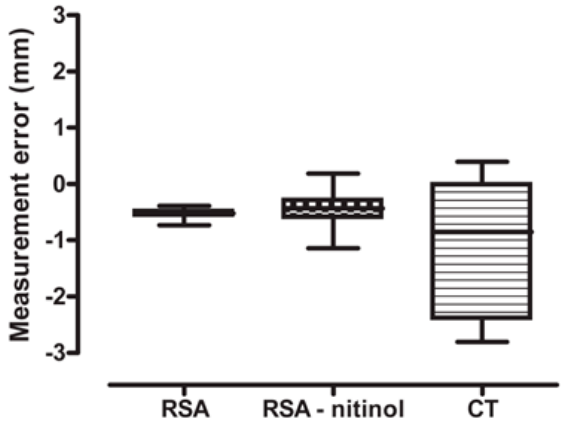

Figure 9. Box plot of the measurement errors of RSA with tantalum aortic markers (RSA), RSA with nitinol endovascular clips as aortic markers (RSA-nitinol), and CT using the renal artery as a reference (CT) compared to the measurement with RSA in a static situation. Median (line), 25th and 75th percentiles (boxes), and range (whiskers) are plotted.

Stent-graft migration was measured with CT under pulsatile flow in the model using the renal artery as a reference. The mean distance of the first migration (n=5) was 6.2±1.22 mm, for a mean (maximum) measurement error of –0.8±1.37 (2.7) mm versus the actual migration. The mean distance of the second migration (n=5) was 12.5±0.88 mm, which gives a mean (maximum) measurement error of–1.4±0.98 (2.8) mm. The pooled measurement error of all migration measurements by CT (n=10) was –1.1±1.17 mm (maximum error 2.8 mm; Figure 9). There appeared to be no significant interobserver variability (p=0.27).

Discussion

This study shows that roentgen stereophotogrammetric analysis is an accurate tool for the measurement of stent-graft migration despite pulsatile motion of the stent-graft and the aortic markers. RSA, with either tantalum or NEC aortic markers, was more accurate than CT with 3D image reconstruction in determining stent-graft migration in our model with physiological pulsatile flow.

The accuracy of CT and RSA in detecting stent-graft migration has been previously assessed in a static plastic model.[9] The measurement error of RSA was 0.002±0.044 mm versus 0.14±0.29 mm for CT with 3D image reconstruction. When comparing these results to the present study, pulsatile movement caused by a simulated cardiac cycle apparently reduces the accuracy of RSA and CT to a measurement error of –0.5±0.16 mm and 1.1±1.17 mm, respectively. Furthermore, in the present study, RSA in the situation with pulsatile motion was less consistent in migration measurement (SD=0.16 mm) compared with RSA in the static situation (SD=0.02/0.03 mm). This may be explained by the limited temporal resolution in imaging. While the RSA images are acquired, the stent and the aorta will have moved slightly, including the renal arteries, the stent-graft markers, and the aortic markers in the wall of the aorta. This results in an image blurring of markers that may lead to less accurate measurement (Figure 10A,B). Furthermore, the stereo RSA images are taken with manually synchronized X-ray tubes; a delay between the 2 roentgen tubes may cause an additional measurement error because of a slight change in marker position between the stereo images (Figure 10C). Nevertheless, this study shows that RSA measurement errors remain extremely small despite pulsatile movement.

The pulsatile movement also occurs during CT acquisition and could partially explain the decrease in accuracy compared to the static experiments as previously described. In the clinical situation, vessel distention (1- to 2-mm diameter change) and craniocaudal (up to 1.5 mm) and rotational (up to 0.59 mm) movements have been described.[16-19] For both the RSA and CT techniques, image acquisition was performed at random time points during the pulsatile cycle. These pulsatile movements may have influenced the accuracy of stent-graft position measurements for both techniques. Electrocardiographically-gated CT has the potential to significantly reduce the measurement error caused by the cyclic motion of the aorta and stent-graft. However, the disadvantages of CT for follow-up after EVAR, such as the high cost and radiation dose, contrast, and logistical burden, remain or may even increase.

An increasing distance between the aortic and stent-graft markers due to migration caused a slight increase in the error of measurement in our study, which is in accord with orthopedic RSA literature.[20] This implies that for the most accurate RSA measurement of stent-graft migration,

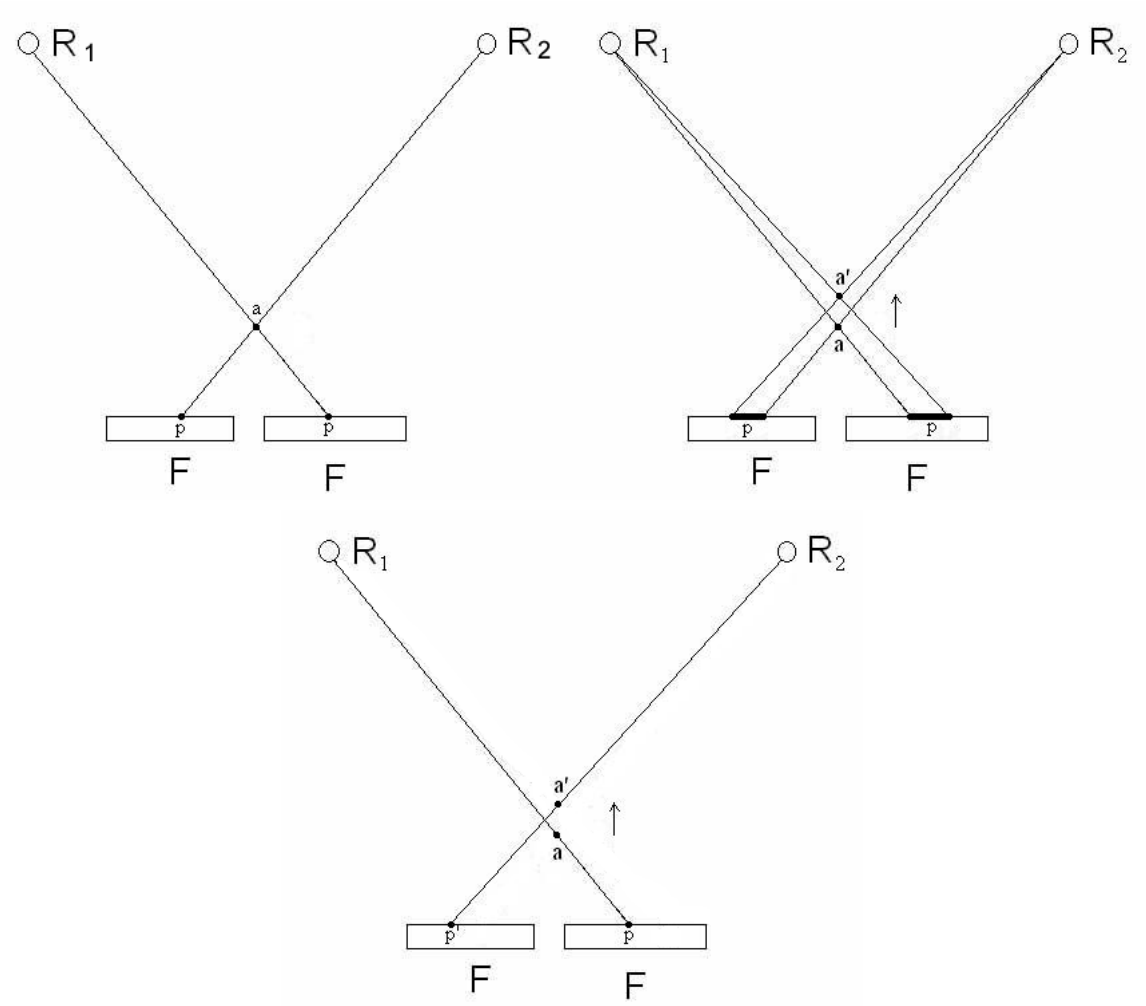

Figure 10. Sources of measurement error in RSA for markers in pulsatile motion versus (**A**) the static situation: marker *a* gives projection *p* on both films *F* after exposure by X-ray foci R_1 and R_2. (**B**) Movement of the marker *a* to *a'* during image acquisition will blur *p*, resulting in less accurate measurement. (**C**) Delay between the exposures of the 2 films *F* will produce 2 different projections, *p* and *p'*, resulting in less accurate measurement.

the aortic markers need to be positioned as close to the stent-graft as possible. Despite the reduction of accuracy after the 13.9-mm migration reported in our study, RSA is still more accurate than CT. A reason for this finding may be the combination of a higher spatial resolution and a shorter acquisition time of an RSA image compared to CT. For these reasons, using a CT scan with less than 64 detectors could further increase the measurement error of CT.

In the present study, we tested an NEC available for use in endovascular surgery for feasibility of use as an aortic marker. The measurement of stent-graft migration using this clip was also accurate but less precise than the standard tantalum markers. This could be explained by the fact that tantalum markers are spherical and have a smaller diameter (Figure 3), which may

be more accurately detected. Despite this decreased accuracy, RSA with NEC aortic markers remained more accurate than CT. Automatic detection of the NECs by the RSA software was not possible due to their non-spherical shape. Manual identification of the center of the marker could be performed without difficulty using the RSA software, from which the position of the marker could be determined. Marker detection is done at a different phase in the processing of RSA images than the migration measurement, and the reviewer was blinded to the amount of migration. Therefore, manual detection of the clip could not interfere with the outcome of measurement. Despite this potential source of error, the RSA measurements using the NEC were accurate. Therefore, the NEC could potentially be used as an aortic marker for RSA measurement in patients. The NEC requires further testing for its clinical suitability as an RSA marker, which is the subject of further study at our institution.

When considering the model, it is apparent that this is not an in vivo situation. Exact reproduction and modeling of cyclic aortic motion remains difficult. Further testing is needed to evaluate the RSA technique and the endovascular clip before patient studies can be undertaken.

Conclusion

RSA is an accurate and feasible tool to measure stent-graft migration in a pulsatile environment. Migration measurement with RSA is more accurate than with 3D image reconstruction of CT scans. Because RSA has several other advantages over CT, it may be a valuable tool for EVAR surveillance. The nitinol clip tested in this study has the potential to be an aortic reference marker in patients.

Acknowledgements

We would like to acknowledge the help of Drs. S.F.G.C. Frerichs and F.E.J.A. Willemssen, Department of Radiology, LUMC, for their participation in the CT analysis. We thank Dr. R. Wolterbeek, DipStatNSS, statistical consultant with the Department of Medical Statistics, LUMC, for his advice and help in the data analysis and M. Boonekamp, Department of Fine Mechanics, and A.A.H. van Immerseel, Department of Anatomy and Embryology, LUMC, for their assistance in building the model. We thank R.M.S. Joemai, BSc, Department of Radiology, LUMC, for his help with the CT data.

References

1. van Marrewijk CJ, Fransen G, Laheij RJ, et al. Is a type II endoleak after EVAR a harbinger of risk? Causes and outcome of open conversion and aneurysm rupture during follow-up. *Eur J Vasc Endovasc Surg*. 2004;27:128-137.

2. Harris PL, Vallabhaneni SR, Desgranges P, et al. Incidence and risk factors of late rupture, conversion, and death after endovascular repair of infrarenal aortic aneurysms: the EUROSTAR experience. *J Vasc Surg*. 2000;32:739-749.

3. Sun Z. Three-dimensional visualization of suprarenal aortic stent-grafts: evaluation of migration in midterm follow-up. *J Endovasc Ther*. 2006;13:85-93.

4. Greenberg RK, Chuter TA, Sternbergh WC, et al. Zenith AAA endovascular graft: intermediate-term results of the US multicenter trial. *J Vasc Surg*. 2004;39:1209-1218.

5. Alric P, Hinchliffe RJ, Wenham PW, Whitaker SC, Chuter TA, Hopkinson BR Lessons learned from the long-term follow-up of a first-generation aortic stent graft. *J Vasc Surg*. 2003;37:367-373.

6. Wolf YG, Hill BR, Lee WA, et al. Eccentric stent graft compression: an indicator of insecure proximal fixation of aortic stent graft. *J Vasc Surg*. 2001;33:481-487.

7. Prinssen M, Buskens E, de Jong Seca, et al. Cost-effectiveness of endovascular versus conventional abdominal aortic aneurysm repair at one year. Results of a randomized trial. In: Prinssen M, ed. DREAM. Oud-Beijerland, The Netherlands: As BV; 2005:89-103.

8. Verhoeven EL, Tielliu IF, Prins TR, et al. Frequency and outcome of re-interventions after endovascular repair for abdominal aortic aneurysm: a prospective cohort study. *Eur J Vasc Endovasc Surg*. 2004;28:357-364.

9. Koning OH, Oudegeest OR, Valstar ER, et al. Roentgen stereophotogrammetric analysis: an accurate tool to assess stent-graft migration. *J Endovasc Ther.* 2006;13:457-467.

10. Karrholm J. Roentgen stereophotogrammetry. Review of orthopedic applications. *Acta Orthop Scand*. 1989;60:491-503.

11. Valstar ER, Vrooman HA, Toksvig-Larsen S, et al. Digital automated RSA compared to manually operated RSA. *J Biomech*. 2000;33:1593-1599.

12. Vrooman HA, Valstar ER, Brand GJ, et al. Fast and accurate automated measurements in digitized stereophotogrammetric radiographs. *J Biomech*. 1998;31:491-498.

13. Valstar ER, de Jong FW, Vrooman HA, et al. Model-based Roentgen stereophotogrammetry of orthopaedic implants. *J Biomech*. 2001;34:715-722.

14. Hinnen JW, Visser MJ, van Bockel JH. Aneurysm sac pressure monitoring: effect of technique on interpretation of measurements. *Eur J Vasc Endovasc Surg* 2005;29:233-238.

15. Valstar ER. Digital roentgen stereophotogrammetry. Development, validation, and clinical application. Thesis, Leiden University. Den Haag, The Netherlands: Pasmans BV, 2001.

16. Stefanadis C, Dernellis J, Vlachopoulos C, et al. Aortic function in arterial hypertension determined by pressure-diameter relation: effects of diltiazem. *Circulation.* 1997;96:1853-1858.

17. Flora HS, Woodhouse N, Robson S, et al. Micromovements at the aortic aneurysm neck measured during open surgery with close-range photogrammetry: implications for aortic endografts. *J Endovasc Ther*. 2001;8:511-520.

18. Verhagen HJ, Teutelink A, Olree M, et al. Dynamic CTA for cutting edge AAA imaging: insights into aortic distensibility and movement with possible consequences for endograft sizing and stent design [Abstract]. *J Endovasc Ther*. 2005;12(suppl I):I-45.

19. Vos AW, Wisselink W, Marcus JT, et al. Cine MRI assessment of aortic aneurysm dynamics before and after endovascular repair. *J Endovasc Ther*. 2003;10:433-439.

20. Spoor CW, Veldpaus FE. Rigid body motion calculated from spatial co-ordinates of markers. *J Biomech*. 1980;13:391-393.